

Comparative Assessment and Multivariate Optimization of Commercially Available Small Scale Reverse Osmosis Membranes

M. C. Garg^{1*} and H. Joshi²

¹Amity Institute of Environmental Sciences (AIES), Amity University Uttar Pradesh, Sector-125, Noida, Uttar Pradesh 201313, India

²Department of Hydrology, Indian Institute of Technology Roorkee, Roorkee, Uttarakhand 247667, India

Received 18 March 2014; revised 9 July 2015; accepted 21 September 2015; published online 27 February 2017

ABSTRACT. Requirement of reverse osmosis (RO) process at places facing energy and water quality problem makes its assessment and optimization vital while considering recovery, rejection as well as specific energy consumption. In the present paper, three thin film composite (TFC) RO membranes (make: CSM, Dow and Vontron) in spiral wound (SW) configuration have been chosen to study their relative performance. Comparative study of RO membranes was conducted using experimental observations supported by membrane characterization. Optimization experiments were performed using central composite design (CCD) of response surface methodology (RSM). Four input variables viz. feed water pH, temperature, pressure and concentration were optimized and interaction between them was observed, while, recovery, rejection and specific energy consumption (SEC) were taken as response attributes. The experiments conducted employing the optimized input values validated the developed RSM model. Predictive model using multiple response optimization revealed the optimal efficiency of CSM RO membrane at 6.53 pH, 1500 mg/L concentration, 0.78 MPa pressure and 31.94°C temperature producing 19.25% water recovery, 89.21% salt rejection and 17.60 kWh/m³ SEC, respectively. Membrane surface characterization was carried out by FE-SEM, AFM, contact angle measurement and FTIR. The lesser contact angle and smoother surface apparently contributed to the better performance of CSM RO membrane. This paper may demonstrate a simple method for optimizing the commercially available small scale RO membranes.

Keywords: brackish groundwater treatment, multivariate optimization, RSM, small scale reverse osmosis membranes, specific energy consumption

1. Introduction

Freshwater problems implying degrading groundwater quality and increasing treatment costs are expected to increase in coming years. The degradation in groundwater quality (geogenic and anthropogenic) at the source level is mainly due to the intensification of agriculture along with non-judicious use of fertilizers and pesticides, addition of solid and liquid wastes and their residuals resulting from rapid urbanization and widespread reduction in recharge of severely strained aquifers to meet ever rising water demands (Champidi et al., 2011). Poor groundwater quality has many economic costs associated with it, one of which is towards the water treatment. Desalination has meanwhile emerged as a solution for locations, where access to water is limited and groundwater has become increasingly saline (UNEP, 2012). Small reverse osmosis (RO) desalination units, mostly installed by the private sector, can now be found as a secondary source of drinking water where municipal supplies are not delivered (World Bank, 2009). Mo-

reover, RO process has been continuously improved for producing drinking water from brackish groundwater and seawater all over the world (Elsaid and Abdel-Wahab, 2012). Commercially available small scale RO process can remove dissolved ions and therefore is well suited for brackish groundwater treatment (Hamouda et al., 2013).

As a higher feed water recovery would result in smaller installation size of the membrane unit as well as have less capital and operating costs, few studies concerning the evaluation and optimization of small scale RO membranes (sufficient for 10 to 25 people in a community) have been carried out that mainly focussed on maximizing water recovery and salt rejection (Elfil et al., 2007; Khayet et al., 2011; Hamouda et al., 2013). In addition, environmental problem and energy crisis in near future will be more obvious due to increasing demand of fossil fuel (Şen, 2004), therefore, the expectation for development of energy conserving RO systems, while maximizing recovery and rejection are more prominent. Application of the small scale RO plants at the areas facing energy challenges such as military operations, catastrophic calamities and natural disasters may be possible. So far, multivariate optimization, characterization and comparison of the commercially available small scale RO systems have not been given much attention and thereby need to be studied. The main objec-

* Corresponding author. Tel.: +91 9760295790; fax: +91 120 4392406.
E-mail address: manoj28280@gmail.com (M. C. Garg).

tives of this work are performance evaluation of the commercially available small scale RO system with an aim to increase water recovery, salt rejection and at the same time to minimize the SEC.

Present paper deals with the optimization and characterization of three commercially available RO membranes used in small scale community level systems in India. Therefore, optimization experiments were carried out to maximize water recovery and salt rejection along with the minimization of energy consumption of small scale brackish water RO process using pH, feed temperature, feed pressure and concentration of feed solution as input parameters. Synthetic water nearly close to actual groundwater was used for all the experiments. Due to the considerable contribution of response surface methodology (RSM) in improving precision and accuracy of estimated optimized values of process variables, it is usually employed for experiment design (Razali et al., 2013). The advantages of RSM include reduction in number of experiments and minimization of experimental cost and time consumption (Ferreira et al., 2007a; Zhao et al., 2014). In the present study, optimization was performed employing RSM using centre composite design (CCD). Furthermore, validation experiment of these membrane results was also conducted as per the obtained optimized value of RSM prediction. Characterization of membranes was carried out by atomic force microscopy (AFM), scanning electron microscopy (FE-SEM), fourier transform infrared spectroscopy (FTIR) and contact angle measurement. A correlation between surface properties and membrane filtration results was obtained.

2. Methods

2.1. Artificial Groundwater Formulation

To evaluate the present groundwater quality situation in India, Delhi region was selected for our study. Groundwater sample was collected from Timarpur, Delhi (India). Analysis of various drinking water quality parameters reveals that the feed water of the RO plant was contaminated in terms of dissolved component comprising primarily of calcium (Ca), magnesium (Mg), chloride (Cl) and sulphate (SO₄) necessitating. Thus, the use of RO treatment plant for this type of water.

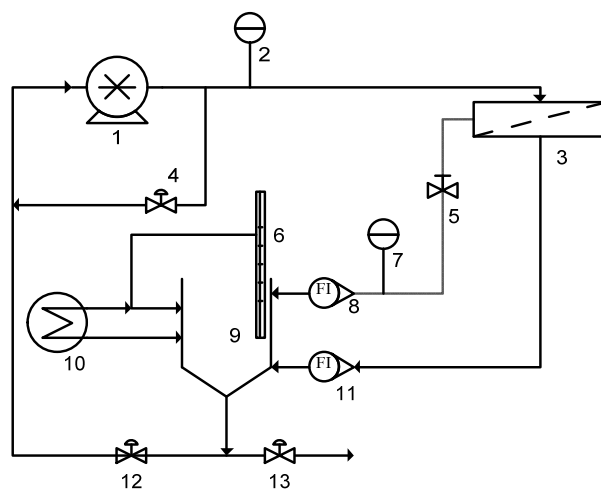
As the laboratory scale RO membrane experiments are generally not practically feasible with actual brackish groundwater due to its inadequate availability and fluctuating quality (Bohdziewicz et al., 1999; Mehdizadeh, 2006; Rahardianto et al., 2007), hence, in the present study, synthetic water was formulated in the laboratory on the basis of major ionic elements of actual groundwater and was further used for performing different experiments. For the formation of synthetic water, a mathematical matrix based computation was employed for estimation of the desired composition of different constituents (Adams and Bubucis, 1998). Based on this formulation, synthetic water was prepared in the laboratory by using analytical grade chemicals (make: Merck, India). Furthermore, to validate the accuracy of this formulation, concentration of elements of the synthetic water were analysed experimentally an-

d compared with that of actual groundwater.

Experimental results of the constituent concentrations of the synthetic groundwater came very close to those (correlation coefficient 0.9982) in actual ground water. This synthetic water was used further in different optimization experiments.

2.2. Experimental Setup and Operational Procedure

A laboratory scale RO membrane system (Make: Permionics membrane Pvt. Ltd., Vadodara, Gujrat, India) was installed to investigate the performance of various spiral wound RO membranes. Figure 1 shows a schematic diagram of the laboratory scale RO system. It consists of a feed water tank, high pressure pump, membrane module consisting of spiral wound RO membrane having 5 cm diameter and 30.5 cm length. Synthetic ground water was used as feed water in all the experiments. The concentration of feed water was in the range of 500 - 4,500 mg/L.



Note: 1 = high pressure pump, 2 = feed pressure gauge, 3 = RO module, 4 = bypass valve, 5 = pressure control valve, 6 = temperature probe, 7 = concentrate pressure gauge, 8 = concentrate flow meter, 9 = feed water tank, 10 = temperature controller, 11 = permeate flow meter, 12 & 13 = valve.

Figure 1. Experimental scheme of laboratory level small scale RO desalination plant.

Feed flow rate was kept constant during experiments by pumping feed water along a feed bypass valve. The system pressure was adjusted using a concentrate valve and monitored by a pressure gauge. Minimum and maximum pressure applied in RO experiments were within the prescribed limits recommended by membrane manufacturers (Table 1). The feed water was pumped to the RO membrane which rejected the dissolved ions from feed water and allowed fresh water to permeate through it.

The concentrate and permeate streams were recycled into the feed water tank for continuous evaluation of the system. After every run, the system was thoroughly rinsed with Milli-Q water for several minutes and completely drained after-

wards. Feed water temperature was kept constant by automatic temperature controlling unit using circulating hot/cold water. 15 mL water samples were collected simultaneously every hour from the feed and permeate. The temperature, pH and electrical conductivity of each of these samples, in addition to the permeate flow rate (from which flux was calculated), were measured.

Optimization experiments were carried out to maximize water recovery, salt rejection and to minimize SEC of small scale brackish water RO process (Joyce et al., 2001) for given feed water pH, temperature, pressure and concentration.

The concentration of anions and cations in samples was estimated using the Ion Chromatograph (Make: Metrohm Ltd., Switzerland). Conductivity meter (Sension, HACH) was used to determine the TDS of feed and permeate water. The salt rejection (%) was calculated using following equation (Mane et al., 2009):

$$\text{Salt rejection}(\%) = \left(1 - \frac{C_p}{C_f}\right) \times 100 \quad (1)$$

where C_f = feed concentration in mg/L, and C_p = product water concentration (mg/L). The feed water recovery (%) was calculated by using following equation (Koutsou et al., 2015):

$$\text{Water recovery}(\%) = \left(\frac{Q_p}{Q_f}\right) \times 100 \quad (2)$$

where Q_p = permeate flow rate (L/h), and Q_f = feed flow rate (L/h). Also, SEC was calculated from the following equation (Zhu et al., 2009):

$$\text{SEC} = \left(\frac{I \times V}{Q_p}\right) \text{ kWh} / \text{m}^3 \quad (3)$$

where SEC is the specific energy consumption in kWh/m³, I = current intensity (A), and V = electrical potential (V) of AC power used to operate the motor.

2.3. Membranes

Three Thin film composite (TFC) RO membranes from three leading manufacturing companies (CSM, Dow and Vontron) in spiral wound configuration were used to perform laboratory scale experiments. Operating specifications of these membranes were used for limiting the range of input parameters for each membrane (Table 1). The membranes were pre-conditioned by soaking in DI water for 2 days, followed by thorough rinsing using DI water prior to testing.

Table 1. Range of Input Variables Taken in Different RO Membranes Experiments

Actual input variables	Coded symbol	Coded level				
		-α	-1	0	+1	+α
CSM						
Temperature (°C)	A	20	24	28	32	36
Pressure (MPa)	B	0.49	0.59	0.69	0.78	0.88
Concentration (mg/L)	C	500	1500	2500	3500	4500
pH	D	5	6	7	8	9
Dow						
Temperature (°C)	A	20	24	28	32	36
Pressure (MPa)	B	0.59	0.88	1.18	1.47	1.77
Concentration (mg/L)	C	500	1500	2500	3500	4500
pH	D	5	6	7	8	9
Vontron						
Temperature (°C)	A	15	20	25	30	35
Pressure (MPa)	B	0.29	0.59	0.88	1.18	1.47
Concentration (mg/L)	C	500	1500	2500	3500	4500
pH	D	5	6	7	8	9

2.4. Experimental Design

To reduce the number of experiments and to minimize the experimental cost and time, RSM is generally employed (Razali et al., 2013).

To determine both linear and quadratic models, CCD based statistical experimental design was used (Idris et al., 2006; Khayet et al., 2011a; Razali et al., 2013; Chakraborty et al., 2014). It combines two level full factorial (cubic) designs (Qin et al., 2008) with additional axial (star) points and a set of centre points at the centre of the experimental region (Wang et al., 2013a). The centre points were repeated to improve the precision of experiments (Bezerra et al., 2008; Ferreira et al., 2007b). During RS modelling, input variables (x_1, x_2, \dots, x_n) in coded scale level vary from the minimum level (-1) up to the maximum level (+1). To determine a critical point (maximum, minimum, or saddle), a second-order model containing quadratic terms is often used and can be presented in a general form as:

$$y = \beta_0 + \sum_{i=1}^n \beta_i x_i + \sum_{i=1}^n \beta_{ii} x_i^2 + \sum_{i < j}^n \beta_{ij} x_i x_j + \varepsilon \quad (4)$$

where y denotes the predicted response, x_i refers to the coded levels of input variables; $\beta_0, \beta_i, \beta_{ii}$ and β_{ij} are the regression coefficients (constant term, linear, quadratic and interaction parameters); n is the number of variables and ε is the experimental error, which is assumed to be random with zero mean (Bezerra et al., 2008; Wang et al., 2013b). In RSM model solution, homogeneity was assumed for all factors that were continuously monitored and regulated (Shuman, 1995). Design Expert software (Stat-Ease Inc., version 7) was used for graphical analysis and model fitting.

In this study, the mutual effect and the relative significance of four input factors on the performance of RO membrane process was investigated by employing RSM with CCD (Kha-yet et al., 2011b). Experiments were carried out for different ranges of concentration, temperature, pH and pressure of feed water (Table 1). A total of 30 experiments were proposed by the design expert software, comprising 16 factorial experiments, 8 axial experiments and 6 replicative experiments at the central point as highlighted in the following equation:

$$N = 2^n + 2n + n_c = 2^4 + (2 \times 4) + 6 = 30 \quad (5)$$

where N is the total number of experiments required, n is the number of numeric factors and n_c is replicate number at the central point. Further, multi-parameter non-linear regression models were developed as actual and coded factors (Montgo-mery, 2004).

Actual and coded values of input variables used in RSM are given in Table 1. RS model was solved for maximizing the water recovery and salt rejection while minimizing SEC. Three dimensional surface plots for response surfaces (RS) were generated from the developed model. Validation experiments were conducted employing the optimal values of the input parameters to verify the predicted values of the RSM.

2.5. Membrane Characterization

Characterization of different RO membranes was carried out by AFM, FE-SEM, FTIR and contact angle measurement. All RO membrane samples were extensively rinsed and immersed in Milli-Q water for 12 hours and dried at room temperature before measurement to confirm the absence of any preservative solution.

2.5.1. Atomic Force Microscopy (AFM)

Surface morphology and roughness of the RO membranes were analysed by AFM analysis (Lalia et al., 2013). It was conducted on a scanning probe microscope (model: NT-MDT NT-EGRA). Tapping mode of scanning was used to analyze the surface roughness of the RO membranes.

2.5.2. Scanning Electron Microscopy (SEM)

SEM (model: ULTRA plus, Carl Zeiss, Germany,) was used to observe the surface structure of the RO membranes (Lalia et al., 2013). Dried samples cut into pieces were put on sample stubs. Sputtering apparatus was used for sputtering a thin layer of gold on these samples. Finally, SEM images of prepared samples were observed at 15 kV and 20,000 × and 30,000 × magnification.

2.5.3. Fourier Transform Infrared (FTIR) Spectrometer

FTIR analysis was performed using a FTIR spectrometer (model: Thermo Fisher Scientific Inc.). Sample of RO membrane was ground and mixed with anhydrous potassium bromide and subsequently pressed into a circular disk. FTIR spec-

tra was obtained for every membrane type, with each spectrum collected from 600 to 4000 cm^{-1} . These spectra were subsequently improved for the penetration depth and background subtraction with the OMNIC software (Ver. 8.0, Thermo Fisher Scientific Inc.).

2.5.4. Contact Angle Measurement

The contact angle of dry and clean RO membrane surfaces was analysed using the sessile drop method to measure the hydrophilicity. A pure water drop (3 ml) was placed on flat RO surface by microsyringe with a stainless steel needle. The contact angle between liquid drop and RO surface was measured by monochrome image, recorded by an interline camera of drop shape analyzer (DSA25, make: KRUSS) connected to a software. Average value of three samples were taken for calculation.

3. Results and Discussion

3.1. RSM and ANOVA Analysis

Analysis of variance (ANOVA) was employed to evaluate the adequacy of the selected model (Wang and Huang, 2014). ANOVA was used to analyse experimental data of RSM. Experimental response models were derived and used to find optimal values of the operating variables. Table 2 shows the CCD experimental design for RO membranes that was developed by Design Expert software (Stat-Ease, Inc, Minneapolis, MN).

3.1.1. Optimization of Water Recovery

Graphical presentation of the data and analysis from RS-M are presented in the form of RS plot. The comparative RS plots for water recovery as a function of different variables are shown in Figure 2(a-f).

As seen in Figure 2(a), at low and high values of temperature, water recovery increases with increase in pressure from 0.59 MPa to 0.79 MPa for CSM membrane. Similar trend is observed for Dow membrane for an increase in pressure (from 0.88 MPa to 1.47 MPa) in Figure 2(b) and 0.59 MPa to 1.18 MPa for Vontron membrane in Figure 2(c). The water recovery increases apparently because higher pressure allows more flow of water through the membrane (Koyuncu et al., 2001; Sassi and Mujtaba, 2010). Effects of feed water concentration and pH on water recovery are not significant for CSM membrane (Figure 2d). However, at low and high pH, water recovery decreases with concentration from 1500 mg/L to 3500 mg/L for Dow and Vontron membranes as shown in Figure 2(e and f). Lower water recovery is apparent because of higher salt concentration, causing the negative effect of concentration polarization and decreasing membrane water flux (Koyuncu et al., 2001). On the other hand, the effect of pH and temperature on water recovery are not significant in these cases because of the low susceptibility of polysulphone membrane to conformational variations in response to changes in temperature and pH (Arkhan-gelsky et al., 2007). The response sur-

Table 2. Experimental Inputs and Responses of CSM, Dow and Vontron RO Membrane

Run	Input variables				Responses								
	A	B	C	D	Recovery (%)			Rejection (%)			SEC (kWh/m ³)		
					CSM	Dow	Vontron	CSM	Dow	Vontron	CSM	Dow	Vontron
1	-1	-1	-1	-1	9.09	8.26	3.12	91.62	89.93	67.11	28.16	29.33	55
2	+1	-1	-1	-1	6.98	10.39	4.23	90.22	89.77	82.59	28	23.39	43.21
3	-1	+1	-1	-1	18.92	12.59	8.88	90.99	84.40	79.07	17.60	24.44	26.79
4	+1	+1	-1	-1	20	16.11	12.39	89.19	85.50	85.58	17.60	19.25	21.11
5	-1	-1	+1	-1	6.98	5.08	2.91	86.60	82.66	70	38.72	42.35	67.22
6	+1	-1	+1	-1	8.84	5.50	3.52	85.14	83.64	80.75	29.94	38.89	53.78
7	-1	+1	+1	-1	14.63	8.59	8.93	83.52	73.07	80.15	26.40	31.21	29.18
8	+1	+1	+1	-1	17.83	11.22	10.63	78.33	76.40	80.99	22.47	25.48	24.87
9	-1	-1	-1	+1	8.16	7.52	3.89	92.02	91.09	72.62	29.04	34.05	50
10	+1	-1	-1	+1	9.09	8.81	5	92.08	90.74	86.21	29.04	27.31	41.72
11	-1	+1	-1	+1	12.79	11.22	9.42	90.11	87.04	79.20	28	26.10	26.79
12	+1	+1	-1	+1	17.65	17.06	12.64	90.03	82.26	82.64	20.53	21.90	20.64
13	-1	-1	+1	+1	7.75	4.71	2.99	85.67	86.12	79.25	35.62	45.83	63.68
14	+1	-1	+1	+1	8.92	5.20	3	86.39	86.18	84.08	32.17	40.10	48.40
15	-1	+1	+1	+1	16.08	8.62	8.34	82.90	79.56	84.85	28.31	35	32.50
16	+1	+1	+1	+1	18.03	9.75	9.12	83.31	81.67	86.42	24	27.84	26.73
17	-α	0	0	0	10	8.17	5.16	89.16	82.81	72.42	29.92	32.13	44.25
18	+α	0	0	0	15	11.35	8.86	87.16	81.91	88.11	20.53	22.34	27.31
19	0	-α	0	0	5.88	3.45	0.85	89.61	87.33	61.26	37.55	46.93	80
20	0	+α	0	0	24.14	16.61	13	84.92	70	75	19.11	30	25.06
21	0	0	-α	0	10.01	12.02	8.59	93.53	87.84	85.31	20.53	20.93	27.31
22	0	0	+α	0	9.09	7.46	5.24	83.90	79.21	82.41	27.20	40	43.50
23	0	0	0	-α	12.82	9.14	6.68	84.27	78.85	86.77	25.34	27.50	34.68
24	0	0	0	+α	9.52	7.51	6.34	90.34	88.77	90.99	30.80	31.09	36.67
25	0	0	0	0	12.20	10.07	6.80	90.12	77.56	85.95	24.64	25.54	35.16
26	0	0	0	0	12.73	8.99	6.98	92.00	82.10	84.72	25.14	25.54	34.22
27	0	0	0	0	13.13	10.07	7.24	88.25	77.56	85	23.69	25.54	32.91
28	0	0	0	0	11.28	8.99	6.89	88.93	82.10	83.91	28	25.54	34.68
29	0	0	0	0	10.53	9.88	6.80	89.96	83.07	85.73	30.80	24.44	35.16
30	0	0	0	0	12.50	9.88	6.72	90.15	83.07	86.43	24.64	24.44	35.65

*A = Temperature, B = Feed Pressure, C = Feed Concentration, D = pH.

face indicates a general trend of enhancement in water recovery with increasing feed pressure. In contrast, water recovery decreases on increasing feed water concentrations.

Table 3 shows the ANOVA results for water recovery of CSM, Dow and Vontron RO membranes. F-values of 26.49, 24.08 and 212.80 for CSM, Dow and Vontron RO membranes respectively imply that the quadratic model is significant. The large P values (> 0.05) show that the F-statistic is insignificant for all RO membranes, implying good correlation between the variables and process responses.

For the CSM RO membrane, ANOVA response for water recovery obtained from the response surface quadratic model shows that model term B is highly significant, whereas terms A, B², C² are significant. A high R² coefficient (close to unity) (Table 3) confirms a satisfactory fit of the quadratic model to the experimental data. The quadratic equation in terms of the coded factors for response on “water recovery” of CSM mem-

brane is given as follows:

$$\begin{aligned}
 \text{Water recovery}_{\text{csm}} = & 12.06 + 0.96(A) + 4.44(B) \\
 & - 0.23(C) - 0.47(D) + 0.58(AB) + 0.21(AC) \\
 & + 0.30(AD) - 0.12(BC) - 0.55(BD) + 0.61(CD) \\
 & + 0.20(A^2) + 0.83(B^2) - 0.54(C^2) - 0.13(D^2)
 \end{aligned} \tag{6}$$

where A is the temperature (°C), B is the pressure (MPa), C is the concentration (mg/L) and D is the pH.

Table 3 shows that the model terms B, C are highly significant, whereas terms A, AB, AC are significant. Note that R² value is about 0.9574, being close to unity, which represents an excellent fit. The quadratic equation in terms of the coded factors for response on “water recovery” of Dow membrane is given as follows:

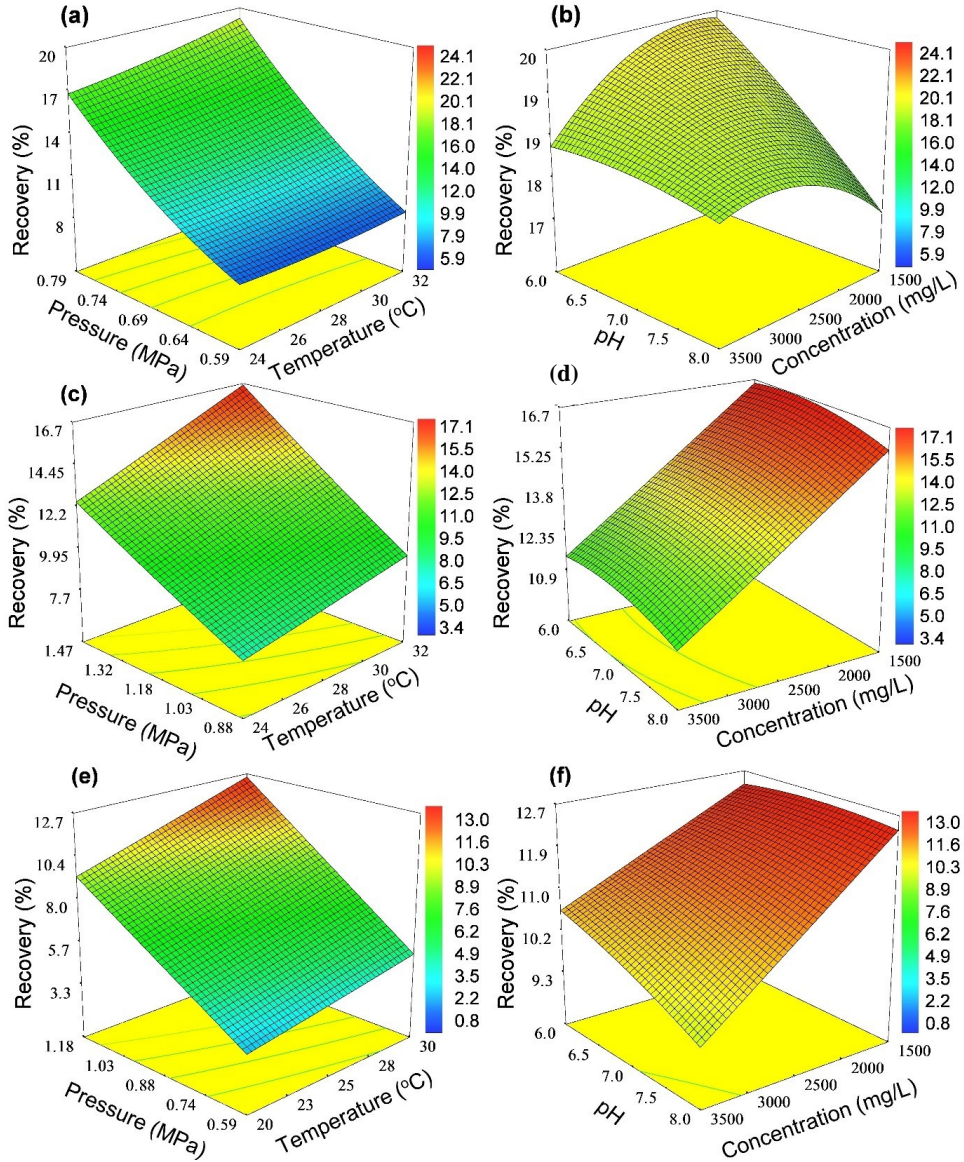


Figure 2. Response surface plots showing the effect of different variables on water recovery of CSM (a, b); Dow (c, d) and Vontron (e, f).

$$\begin{aligned}
 \text{Water recovery}_{Dow} = & 9.65 + 0.99(A) + 2.75(B) \\
 & - 1.77(C) - 0.34(D) + 0.55(AB) - 0.51(AC) \\
 & + 2.57E - 0.03(AD) - 0.27(BC) + 0.070(BD) \\
 & + 0.038(CD) + 0.019(A^2) + 0.087(B^2) \\
 & + 0.014(C^2) - 0.34(D^2)
 \end{aligned} \quad (7)$$

For the Vontron RO membrane, the ANOVA response for water recovery obtained from the response surface quadratic model shows that the model terms A , B , C are highly significant, whereas terms AB , AC , BC and CD are significant.

The R^2 value of 0.9949 (99.49%) represents an excellent fit of the regression model for water recovery of Vontron membrane (Table 3). The quadratic equation in terms of coded factors for response on “water recovery” of Vontron membrane, is given as follows:

$$\begin{aligned}
 \text{Water recovery}_{Vontron} = & 6.90 + 0.81(A) + 3.17(B) \\
 & - 0.70(C) - 0.037(D) + 0.40(AB) - 0.37(AC) \\
 & - 0.11(AD) - 0.16(BC) - 0.15(BD) - 0.30(CD) \\
 & + 0.022(A^2) + 5.36E - 0.04(B^2) - 1.48E \\
 & - 0.03(C^2) - 0.1(D^2)
 \end{aligned} \quad (8)$$

Table 3. ANOVA Result for RS Quadratic Model for Different Input Variables

Input Variables	Membranes	Source	Sum of Squares	DF	Mean Square	F Value	P > F	R ²
Water Recovery	CSM RO	Model	553.6266	14	39.5447	26.4869	< 0.0001**	0.9611
		Lack of Fit	17.6326	10	1.7632	1.8513	0.2576#	
	Dow RO	Model	296.9527	14	21.2109	24.0834	< 0.0001**	0.9574
		Lack of Fit	11.8829	10	1.1882	4.4741	0.0560#	
Salt Rejection	Vontron RO	Model	275.6002	14	19.6857	212.8065	< 0.0001**	0.9949
		Lack of Fit	1.2166	10	0.1216	3.5595	0.0869#	
	CSM RO	Model	333.2824	14	23.8058	13.1467	< 0.0001**	0.9246
		Lack of Fit	18.9688	10	1.8968	1.1576	0.4628#	
SEC	Dow RO	Model	659.8309	14	47.1307	7.1681	0.0003*	0.8699
		Lack of Fit	63.9939	10	6.3993	0.9239	0.5740#	
	Vontron RO	Model	1279.2510	14	91.3750	34.1751	< 0.0001**	0.9696
		Lack of Fit	35.8749	10	3.5874	4.2395	0.0622#	
SEC	CSM RO	Model	751.8794	14	53.7056	10.1417	< 0.0001**	0.9044
		Lack of Fit	42.7727	10	4.2772	0.5833	0.7811#	
	Dow RO	Model	1598.1530	14	114.1538	132.5644	< 0.0001**	0.9919
		Lack of Fit	11.3289	10	1.1328	3.5674	0.0865#	
Vontron RO	Model	5865.0270	14	418.9305	215.7788	< 0.0001**	0.9950	
	Lack of Fit	24.3826	10	2.4382	2.5722	0.1544#		

DF: Degree of freedom, ** = Highly significant, * = Significant, # = Not significant.

3.1.2. Optimization of Salt Rejection

Three dimensional comparative RS plots for salt rejection as a function of different input variables are depicted in Figure 3. At high and low values of temperature, the salt rejection does not show any significant change with pressure for either CSM or Dow membranes. However, it increases at a low value of pressure (0.59 MPa) with temperature ranging from 20 °C to 30 °C for Vontron membrane (Figure 3e). This is apparently because higher diffusion rate of solute through the membrane is possible as the solubility increases with temperature (Arora et al., 2004; Gedam et al., 2012). Similarly, at high and low values of temperature, salt rejection increases with the pressure from 0.59 MPa to 1.03 MPa for Vontron membrane. This is because the rejection increases along with operating pressure due to the higher formation of concentration polarization at the membrane interface (Tu et al., 2010; Zulkali et al., 2005). At low values of pH, salt rejection decreases with feed water concentration that ranges from 1500 mg/L to 3500 mg/L for all three RO membranes (Figures 3b, 3d, and 3f). This is because at high feed salinity, the salt passage increases (Bartels et al., 2005). However, at high values of pH, the salt rejection does not show any significant change with feed water concentration for all RO membranes.

This analysis shows that the salt rejection in a small scale RO plant would be better at low feed concentration, low pH and high pressure. CSM (89.2%) and vontron (89.66%) among the three RO membranes show the better performance for the salt rejection.

In Table 3, ANOVA results show F-values of 13.14, 7.16 and 34.17 for salt rejection of CSM, Dow and Vontron RO membranes. This implies that the quadratic model is significant. The large P values (> 0.05) shows that the F-statistic

values are insignificant for all RO membranes, implying significant model correlation between the variables and process responses.

For the CSM RO membrane, ANOVA response for salt rejection obtained from the response surface quadratic model shows that the model term *C* is highly significant, whereas terms *B*, *D*, *AD*, *B*² and *D*² are significant. Note that *R*² value is about 0.9246, being close to unity, which represents an excellent fit (Table 3). Through multiple regression analysis on the experimental data (Wang and Huang, 2015), response for the salt rejection of CSM RO membranes may be predicted by the following second-order polynomial equation in term of coded values:

$$\begin{aligned} \text{Salt rejection}_{\text{csm}} = & 89.90 - 0.53(A) - 1.28(B) \\ & - 3.07(C) + 0.79(D) - 0.29(AB) - 0.14(AC) \\ & + 0.69(AD) - 0.63(BC) + 0.11(BD) + 0.15(CD) \\ & - 0.51(A^2) - 0.74(B^2) - 0.38(C^2) - 0.73(D^2) \end{aligned} \quad (9)$$

where *A* is the temperature (°C), *B* is the pressure (MPa), *C* is the concentration (mg/L) and *D* is the pH.

For the Dow RO membrane, ANOVA response for salt rejection obtained from the response surface quadratic model shows that model terms *B*, *C* are highly significant, whereas terms *D*, *C*² and *D*² are significant. A high *R*² coefficient (close to unity) (Table 3) confirms a satisfactory fit of the quadratic model to the experimental data. The quadratic equation in terms of the coded factors for response on “salt rejection” of Dow membrane is given as follows:

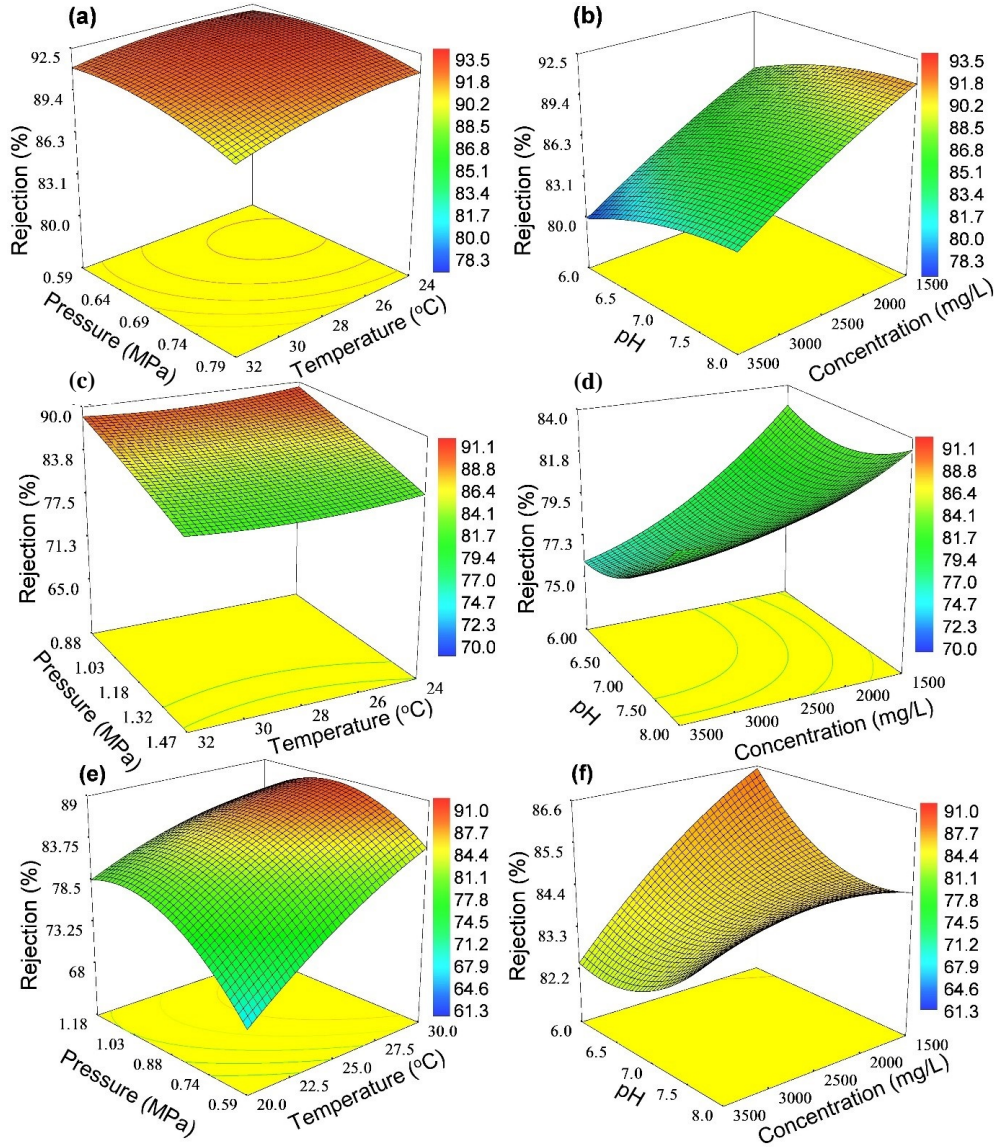


Figure 3. Response surface plots showing the effect of different variables on salt rejection of CSM (a, b); Dow (c, d) and Vontron (e, f).

$$\begin{aligned}
 \text{Salt rejection}_{Dow} = & 80.91 + 0.022(A) - 3.54(B) \\
 & - 2.86(C) + 1.63(D) + 0.077(AB) + 0.67(AC) \\
 & - 0.51(AD) - 0.35(BC) + 0.19(BD) + 1.01(CD) \\
 & + 0.74(A^2) - 0.18(B^2) + 1.04(C^2) + 1.11(D^2)
 \end{aligned} \tag{10}$$

For the Vontron RO membrane, ANOVA response for salt rejection obtained from the response surface quadratic model shows that the model terms A , B , B^2 are highly significant, whereas terms D , AB , AC , BD , CD , A^2 and D^2 are significant. The R^2 value of 0.9696 (close to unity) confirms a satisfactory fit of the quadratic model to the experimental data (Table 3). The quadratic equation in terms of the coded factors for re-

sponse on “salt rejection” of Vontron membrane is given as follows:

$$\begin{aligned}
 \text{Salt rejection}_{Vontron} = & 85.29 + 3.68(A) + 2.66(B) \\
 & + 0.24(C) + 1.56(D) - 2.02(AB) - 1.31(AC) \\
 & - 0.64(AD) + 0.023(BC) - 0.90(BD) + 1.02(CD) \\
 & - 1.29(A^2) - 4.32(B^2) - 0.39(C^2) + 0.87(D^2)
 \end{aligned} \tag{11}$$

3.1.3. Optimization of SEC

The RS plots in Figure 4 illustrate the effect of temperature, pressure, pH and concentration on SEC for all the three RO membranes. At low and high temperature of feed water,

SEC decreases with pressure from 0.59 MPa to 0.79 MPa for CSM membrane, from 0.88 MPa to 1.32 MPa for Dow membrane and from 0.59 MPa to 1.18 MPa for Vontron membrane (Figures 4a, 4c and 4e). This is because the permeate flow rate and the recovery increases at the same time as the applied pressure increases. Also, a decrease in SEC compensates largely for the energy required to apply a higher desalination pressure (Laborde et al., 2001). At a low and high value of pH, SEC increases with concentration ranging from 1500 mg/L to 3500 mg/L for all three RO membranes (Figures 4b, 4d, and 4f). This trend has been observed because the minimum value of required energy increases linearly as a function of the solution concentration (Laborde et al., 2001). It is considerable to note that the high rejection of Vontron membrane as compared to the other membranes results in higher concentration polarization, higher osmotic pressure and consequently lower flux which directly influences SEC (Richards et al., 2011). Based on the above analysis, it may be predicted that small scale RO plants show a low SEC at higher pressure and lesser feed concentration.

ANOVA results presented in Table 3 show F-values of 10.14, 132.56 and 215.77 for SEC of CSM, Dow and Vontron RO membranes. This implies that the quadratic model is significant. The large P values (> 0.05) show that the F-statistic values are insignificant for all RO membranes, implying good correlation between the variables and process responses. Table 3 shows that the model term *B* is highly significant, whereas *C* and *D* are significant terms. A high R^2 coefficient (close to unity) confirms a satisfactory fit of the quadratic model to the experimental data. Through multiple regression analysis on the experimental data, response for the SEC of CSM RO membranes may be predicted by the following second-order polynomial equation in term of coded values:

$$SEC_{csm} = 26.15 - 1.95(A) - 4.28(B) + 2.21(C) + 1.20(D) - 0.21(AB) - 0.80(AC) - 0.15(AD) - 0.30(BC) + 0.98(BD) - 0.79(CD) - 0.089(A^2) + 0.69(B^2) - 0.43(C^2) + 0.62(D^2) \quad (12)$$

where *A*, *B*, *C* and *D* are the coded variables for temperature, pressure, concentration and pH, respectively.

Table 3 shows that model terms *A*, *B*, *C*, *D*, *BC*, *B²*, *C²*, *D²* are highly significant, whereas term *A²* is significant. Note that R^2 value is about 0.9919, which being close to unity, represents an excellent fit of the regression model for SEC of Dow membrane. The quadratic equation in terms of the coded factors for response on “SEC” of Dow membrane is given as follows:

$$SEC_{Dow} = 25.17 - 2.66(A) - 4.33(B) + 4.96(C) + 1.29(D) - 0.026(AB) - 1.663E - 0.04(AC) - 0.22(AD) - 1.58(BC) - 0.18(BD) - 0.13(CD) + 0.42(A^2) + 3.23(B^2) + 1.23(C^2) + 0.93(D^2) \quad (13)$$

For the Vontron RO membrane, ANOVA response for SEC obtained from the response surface quadratic model (Table 3) shows that the model terms *A*, *B*, *C*, *B²* are highly significant, whereas terms *AB*, *BC* and *BD* are significant. The R^2 value of 0.9950 (99.5%) represents an excellent fit of the regression model for SEC of Vontron membrane. The quadratic equation in terms of coded factors for response on “SEC” of Vontron membrane is given as follows:

$$SEC_{Vontron} = 34.63 - 4.36(A) - 13.51(B) + 3.90(C) - 0.28(D) + 1.68(AB) - 0.43(AC) - 0.016(AD) - 1.58(BC) + 1.26(BD) + 0.20(CD) + 0.23(A^2) + 4.41(B^2) + 0.13(C^2) + 0.20(D^2) \quad (14)$$

3.2. Multiple Response Optimization

Membrane optimisation was carried out by the RSM through regression analysis to achieve the maximum recovery, highest salt rejection and the lowest SEC. Predicted numerical optimization of input parameters was obtained and is presented in Table 4. Model predictions validated by the confirmation run at these optimal process conditions, are in agreement with the predicted responses. Less than 6% error for each response showed the reliability of CCD optimisation process. These results demonstrate an improvement in the individual RO membrane employing optimized input parameters. It can be easily concluded by the above analysis that CSM RO membrane shows the best performance at 31.92 °C temperature, 0.78 MPa pressure, 1500 mg/L feed salt concentration and 6.53 pH (very near to the actual i.e. 6.7) with 20.24% water recovery, 90.22% salt rejection and 17.87 kWh/m³ of SEC (Table 4), as compared to Dow and Vontron RO membranes.

Removal efficiency of major ions of validation experiments was studied for divalent ions (93.95% Ca²⁺, 94.10% Mg²⁺ and 94.7% SO₄²⁻) and it was found to be higher as compared to monovalent ions (89.94% Na⁺, 92.02% Cl⁻, 82.15% NO₃⁻, 87.15% HCO₃⁻).

3.3. Membrane Characterization

Surface characterization was carried out by different measurement techniques. Surface roughness of three RO membranes were measured by AFM analysis as shown in Figure 5. The in-plane *x* and *y* scales are 10 μm × 10 μm (1 μm/div), while the *z* axis varies with respect to the surface roughness. AFM analysis reveals that the RMS (Rq) roughness value of the RO membranes varies from 35 μm to nearly 55 μm. The CSM RO membrane was found to be the smoothest, with an RMS (Rq) value of 33.99 μm. Total surface area of the membrane increases with surface roughness which leads to the accumulation of foulants at the ridge-valley structure of the surface. The AFM technique has proved that rough surfaces are more vulnerable to fouling which causes decline in flux and salt rejection (Vrijenhoek et al., 2001).

SEM images of all virgin RO membranes exhibited typi-

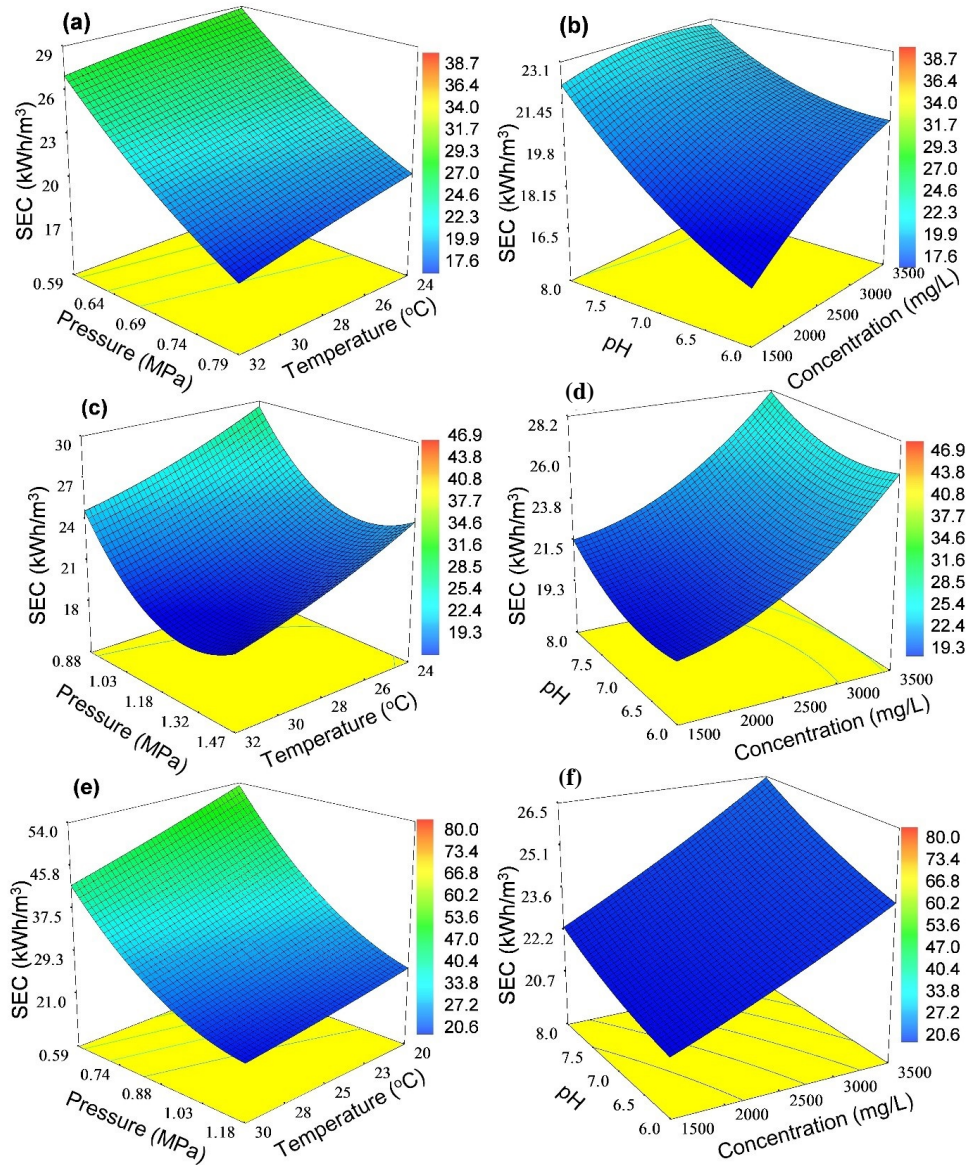


Figure 4. Response surface plots showing the effect of different variables on SEC of CSM (a, b); Dow (c, d) and Vontron (e, f).

Table 4. Multiple Response Optimizations with RSM of Different RO Membranes

Parameter	Optimized input parameter				RSM prediction			Confirmation experiment under optimized conditions		
	Temperature (°C)	Feed Pressure (MPa)	Feed Concentration (mg/L)	pH	Recovery (%)	Rejection (%)	SEC (kWh/M ³)	Recovery (%)	Rejection (%)	SEC (kWh/M ³)
CSM	31.92	0.78	1500	6.53	19.25	89.2	17.6	20.24	90.22	17.87
Dow	32	1.43	1500	6.14	16.1	82.53	18.99	17.12	82.42	19.3
Vontron	30	1.18	1518	6.73	12.75	89.66	19.02	13.37	91.17	20.04

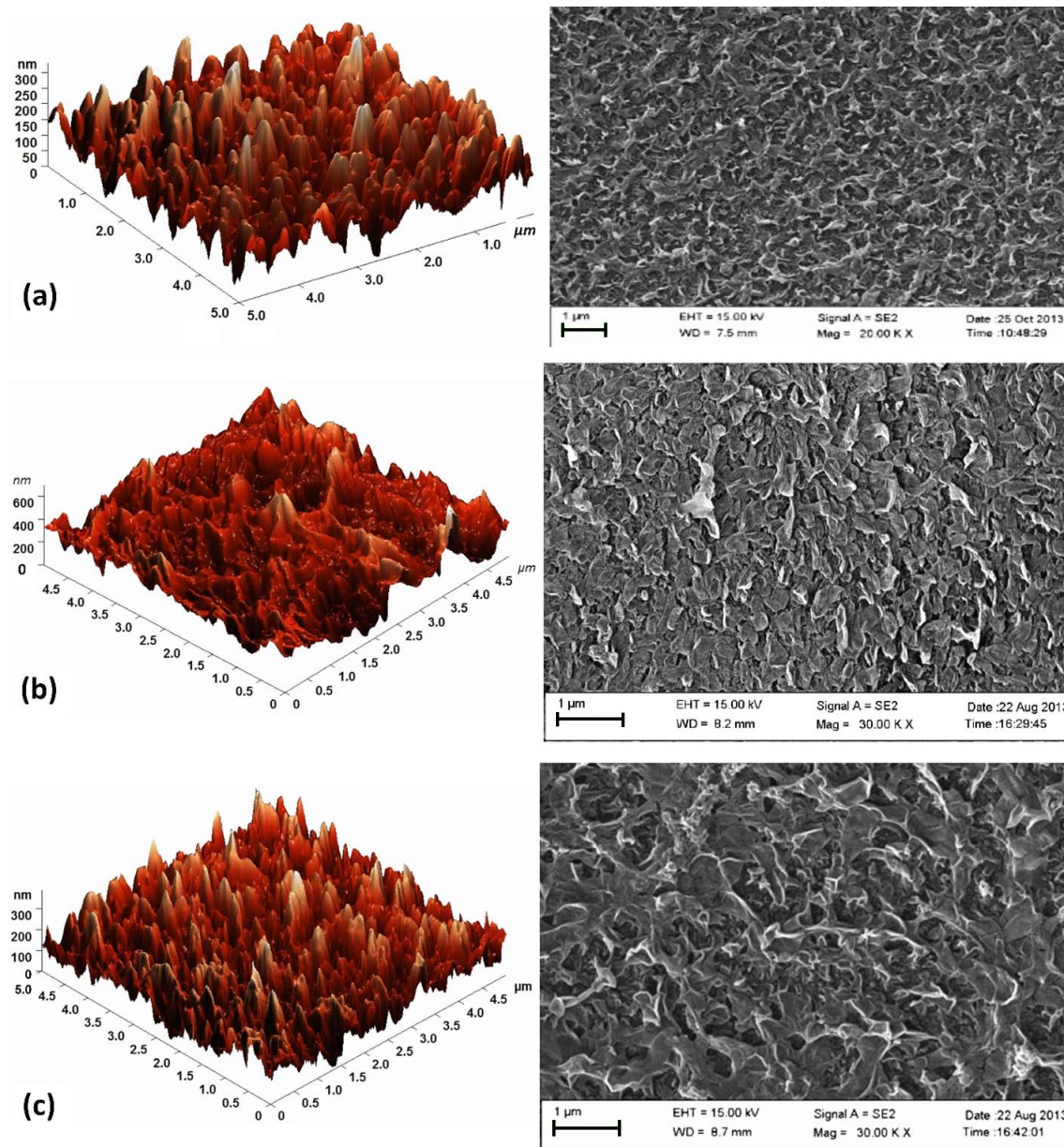


Figure 5. AFM and FE-SEM images of different RO membrane (a) CSM (b) Dow and (c) Vontron.

cal symmetric morphology with no significant difference as shown in Figure 5.

In order to authenticate functional groups on the membrane surfaces, FTIR analysis spectra were obtained for each virgin membranes and shown in Figure 6. These spectra are of wave numbers ranging between 500 and 4000 cm^{-1} . The broad band around 3435.36 cm^{-1} is a complex one due to the overlapping of stretching vibration of N-H and carboxylic groups and additional groups (such as O-H groups) from the coating layer.

Also, IR spectra of all RO membranes were observed to be very similar to the poly (aryl) ether as shown in Figure 6.

Therefore, it can be predicted that top layer of all RO membranes would be constituted of polyether sulphone.

Membrane hydrophilic-hydrophobic properties are based on a contact angle between the liquid-gas tangent and membrane-liquid boundary (Tarboush et al., 2008). Usually RO membrane materials having high contact angle are prone to adsorption of the various solutes. In this study, contact angle analysis was carried out by drop shape analyzer instrument (DSA25, make: KRUSS).

It had been shown earlier that RO membrane fouling, improved flux during operation and the surface roughness are strongly correlated to each other, The hydrophilic RO mem-

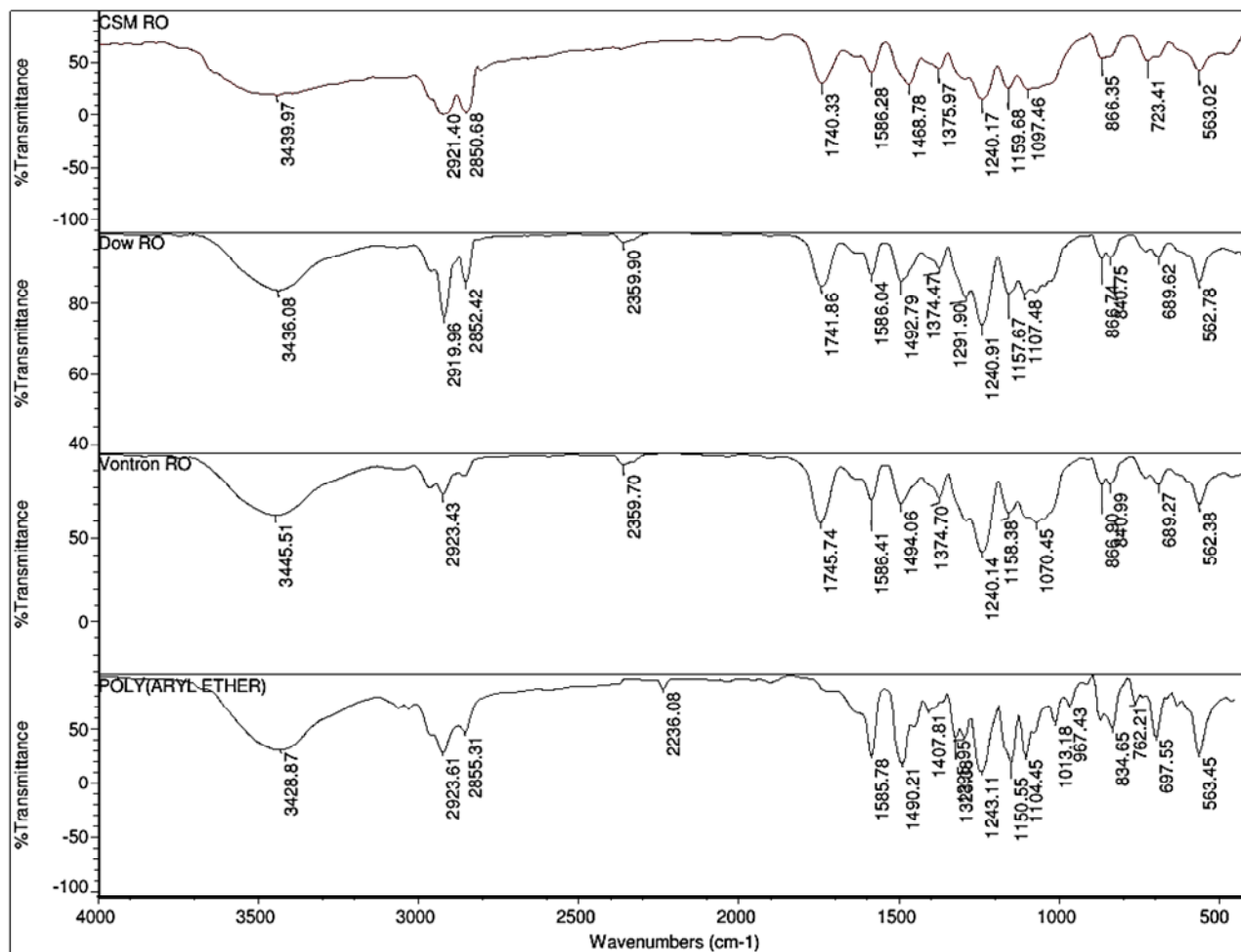


Figure 6. FTIR spectra of virgin CSM, Dow and Vontron RO membranes matched with the spectra of poly (aryl ether).

branes with smoother surfaces are less prone to adsorption of various solutes (inorganic fouling) compared to the relatively more hydrophobic and rougher membranes (Elimelech et al., 1997). The smaller contact angle (higher hydrophilicity) and smoother surface (Lowest RMS value) of CSM RO membrane might be the reason of its better performance.

4. Conclusions

It is necessary to optimize the small scale RO membranes in terms of recovery, rejection along with specific energy consumption. Optimization experiments by using CCD of RSM reveals that among all three commercial RO membranes, CSM membrane showed the best performance and the optimal conditions obtained were 6.53 pH, 1500 mg/L concentration, 0.78 MPa pressure and 31.94 °C temperature with the predicted results of water recovery, salt rejection and SEC of 19.25%, 89.21% and 17.60 kWh/m³, respectively. FE-SEM, AFM, contact angle measurement and FTIR proved to be valuable tools for characterization of RO membrane surface. When used together, these characterization tools provided str-

ong explanation for better performance of small scale RO membranes. From FTIR analysis, it could be predicted that top layer of all RO membranes may be made from polyether sulphone. The lesser contact angle and smoother surface further contributed to the better performance of CSM RO membrane.

The presented methodology highlights a desirable approach for optimizing different RO membranes available in the market to make the RO systems economically viable and efficient.

Acknowledgments. This work was carried out by the financial support given by Ministry of Drinking Water and Sanitation, New Delhi, India under letter no. W-11035/24/2010-WQ (R&D)-TS. We would also like to thank all those involved in this project.

References

- Adams, G., and Bubucis, P. (1998). Calculating an artificial sea water formulation using spreadsheet matrices. *Aquar. Sci. and conserv.*, 2(1), 35-41. <http://dx.doi.org/10.1023/A:1009624710083>
- Arkhangelsky, E., Kuzmenko, D., and Gitis, V. (2007). Impact of ch-

- emical cleaning on properties and functioning of polyethersulfone membranes. *J. Membr. Sci.*, 305(1-2), 176-184. <http://dx.doi.org/10.1016/j.memsci.2007.08.007>
- Arora, M., Maheshwari, R.C., Jain, S.K., and Gupta, A. (2004). Use of membrane technology for potable water production. *Desalination*, 170(2), 105-112. <http://dx.doi.org/10.1016/j.desal.2004.02.096>
- Bartels, C., Franks, R., Rybar, S., Schierach, M., and Wilf, M. (2005). The effect of feed ionic strength on salt passage through reverse osmosis membranes. *Desalination*, 184(1-3), 185-195. <http://dx.doi.org/10.1016/j.desal.2005.04.032>
- Bezerra, M.A., Santelli, R.E., Oliveira, E.P., Villar, L.S., and Escalera, L.A. (2008). Response surface methodology (RSM) as a tool for optimization in analytical chemistry. *Talanta*, 76(5), 965-977. <http://dx.doi.org/10.1016/j.talanta.2008.05.019>
- Bohdziewicz, J., Bodzek, M., and Wąsik, E. (1999). The application of reverse osmosis and nanofiltration to the removal of nitrates from groundwater. *Desalination*, 121(2), 139-147. [http://dx.doi.org/10.1016/S0011-9164\(99\)00015-6](http://dx.doi.org/10.1016/S0011-9164(99)00015-6)
- Chakraborty, S., Dasgupta, J., Farooq, U., Sikder, J., Drioli, E., and Curcio, S. (2014). Experimental analysis, modeling and optimization of chromium (VI) removal from aqueous solutions by polymer enhanced ultrafiltration. *J. Membr. Sci.*, 456(0), 139-154. <http://dx.doi.org/10.1016/j.memsci.2014.01.016>
- Champidi, P., Stamatis, G., and Zagana, E. (2011). Groundwater quality assessment and geogenic and anthropogenic effect estimation in Erasinos Basin (E. Attica). *Eur. Water*, 33, 11-27
- Elfil, H., Hamed, A., and Hannachi, A. (2007). Technical evaluation of a small-scale reverse osmosis desalination unit for domestic water. *Desalination*, 203(1-3), 319-326. <http://dx.doi.org/10.1016/j.desal.2006.03.530>
- Elimelech, M., Xiaohua, Z., Childress, A.E., and Seungkwan, H. (1997). Role of membrane surface morphology in colloidal fouling of cellulose acetate and composite aromatic polyamide reverse osmosis membranes. *J. Membr. Sci.*, 127(1), 101-109. [http://dx.doi.org/10.1016/S0376-7388\(96\)00351-1](http://dx.doi.org/10.1016/S0376-7388(96)00351-1)
- Elsaid, K., Bensalah, N., and Abdel-Wahab, A. (2012). Inland desalination: Potentials and challenges, in Z. N. A. S. Naveed (Ed.), *Advances in Chemical Engineering*, InTech.
- Ferreira, S.L.C., Bruns, R.E., da Silva, E.G.P., dos Santos, W.N.L., Quintella, C.M., David, J.M., de Andrade, J.B., Breikreitz, M.C., Jardim, I.C.S.F., and Neto, B.B. (2007a). Statistical designs and response surface techniques for the optimization of chromatographic systems. *J. Chromatogr.*, 1158(1-2), 2-14. <http://dx.doi.org/10.1016/j.chroma.2007.03.051>
- Ferreira, S.L.C., Bruns, R.E., da Silva, E.G.P., dos Santos, W.N.L., Quintella, C.M., David, J.M., de Andrade, J.B., Breikreitz, M.C., Jardim, I.C.S.F. and Neto, B.B. (2007b). Statistical designs and response surface techniques for the optimization of chromatographic systems. *J. Chromatogr.*, 1158(1-2), 2-14. <http://dx.doi.org/10.1016/j.chroma.2007.03.051>
- Gedam, V.V., Patil, J.L., Kagne, S., Sirsam, R.S., and Labhasetwar, P. (2012). Performance evaluation of polyamide reverse osmosis membrane for removal of contaminants in ground water collected from Chandrapur district. *J. Membr. Sci. Technol.*, 2(3), 2-5. <http://dx.doi.org/10.4172/2155-9589.1000117>
- Hamouda, S.B., Akhtar, F.H., and Elfil, H. (2013). Diagnosis of small capacity reverse osmosis unit for desalinated tap water. *Desalination Water Treat.*, 1-9. <http://dx.doi.org/10.1080/19443994.2013.822334>
- Idris, A., Kormin, F., and Noordin, M.Y. (2006). Application of response surface methodology in describing the performance of thin film composite membrane. *Sep. Purif. Technol.*, 49(3), 271-280. <http://dx.doi.org/10.1016/j.seppur.2005.10.010>
- Joyce, A., Loureiro, D., Rodrigues, C., and Castro, S. (2001). Small reverse osmosis units using PV systems for water purification in rural places. *Desalination*, 137(1-3), 39-44. [http://dx.doi.org/10.1016/S0011-9164\(01\)00202-8](http://dx.doi.org/10.1016/S0011-9164(01)00202-8)
- Khayet, M., Cojocar, C., and Essalhi, M. (2011). Artificial neural network modeling and response surface methodology of desalination by reverse osmosis. *J. Membr. Sci.*, 368, 202-214. <http://dx.doi.org/10.1016/j.memsci.2010.11.030>
- Khayet, M., Cojocar, C., and Essalhi, M. (2011a). Artificial neural network modeling and response surface methodology of desalination by reverse osmosis. *J. Membr. Sci.*, 368(1-2), 202-214. <http://dx.doi.org/10.1016/j.memsci.2010.11.030>
- Khayet, M., Cojocar, C., and Essalhi, M. (2011b). Artificial neural network modeling and response surface methodology of desalination by reverse osmosis. *J. Membr. Sci.*, 368(1-2), 202-214. <http://dx.doi.org/10.1016/j.memsci.2010.11.030>
- Koutsou, C.P., Karabelas, A.J., and Kostoglou, M. (2015). Membrane desalination under constant water recovery -- The effect of module design parameters on system performance. *Sep. Purif. Technol.*, 147(0), 90-113. <http://dx.doi.org/10.1016/j.seppur.2015.04.012>
- Koyuncu, I., Yazgan, M., Topacik, D., and Sarikaya, H.Z. (2001). Evaluation of the low pressure RO and NF membranes for an alternative treatment of Buyukcekmece Lake. *Water Sci. Technol. Water Supply*, 1(1), 107-115
- Laborde, H.M., França, K.B., Neff, H., and Lima, A.M.N. (2001). Optimization strategy for a small-scale reverse osmosis water desalination system based on solar energy. *Desalination*, 133(1), 1-12. [http://dx.doi.org/10.1016/S0011-9164\(01\)00078-9](http://dx.doi.org/10.1016/S0011-9164(01)00078-9)
- Lalia, B.S., Kochkodan, V., Hashaikh, R., and Hilal, N. (2013). A review on membrane fabrication: Structure, properties and performance relationship. *Desalination*, 326(0), 77-95. <http://dx.doi.org/10.1016/j.desal.2013.06.016>
- Mane, P.P., Park, P.K., Hyung, H., Brown, J.C., and Kim, J.H. (2009). Modeling boron rejection in pilot- and full-scale reverse osmosis desalination processes. *J. Membr. Sci.*, 338(1-2), 119-127. <http://dx.doi.org/10.1016/j.memsci.2009.04.014>
- Mehdizadeh, H. (2006). Membrane desalination plants from an energy-exergy viewpoint. *Desalination*, 191(1-3), 200-209. <http://dx.doi.org/10.1016/j.desal.2005.06.037>
- Montgomery, D.C. (2004). *Design and Analysis of Experiments*, Wiley, New York.
- Qin, X.S., Huang, G.H., and Chakma, A. (2008). Modeling groundwater contamination under uncertainty: A factorial-design-based stochastic approach. *J. Environ. Inf.*, 11(1), 11-20.
- Rahardianto, A., Gao, J., Gabelich, C.J., Williams, M.D., and Cohen, Y. (2007). High recovery membrane desalting of low-salinity brackish water: Integration of accelerated precipitation softening with membrane RO. *J. Membr. Sci.*, 289(1-2), 123-137. <http://dx.doi.org/10.1016/j.memsci.2006.11.043>
- Razali, N.F., Mohammad, A.W., Hilal, N., Leo, C.P., and Alam, J. (2013). Optimisation of polyethersulfone/polyaniline blended membranes using response surface methodology approach. *Desalination*, 311(0), 182-191. <http://dx.doi.org/10.1016/j.desal.2012.11.033>
- Richards, L.A., Richards, B.S., and Schäfer, A.I. (2011). Renewable energy powered membrane technology: Salt and inorganic contaminant removal by nanofiltration/reverse osmosis. *J. Membr. Sci.*, 369(1-2), 188-195. <http://dx.doi.org/10.1016/j.memsci.2010.11.06>
- Sassi, K.M., and Mujtaba, I.M. (2010). Simulation and optimization of full scale reverse osmosis desalination plant, in S. Pierucci and G. B. Ferraris (Eds.), *Computer Aided Chemical Engineering*, vol. 28, pp. 895-900, Elsevier.
- Şen, Z. (2004). Solar energy in progress and future research trends. *Prog. Energy Combust. Sci.*, 30(4), 367-416. <http://dx.doi.org/10.1016/j.seppur.2005.10.010>

- 1016/j.peccs.2004.02.004
- Shuman, B. (1995). *A Comparison of Response Surface Methodology and a One-factor-at-a-time Approach as Calibration Techniques for the Bioplume-II Simulation Model of Contaminant Degradation*, Master degree of Science in Engineering and Environmental Management, Air Force Institute of Technology, Air University.
- Tarboush, B.J.A., Rana, D., Matsuura, T., Arafat, H.A., and Narbaitz, R.M. (2008). Preparation of thin-film-composite polyamide membranes for desalination using novel hydrophilic surface modifying macromolecules. *J. Membr. Sci.*, 325(1), 166-175. <http://dx.doi.org/10.1016/j.memsci.2008.07.037>
- Tu, K.L., Nghiem, L.D., and Chivas, A.R. (2010). Boron removal by reverse osmosis membranes in seawater desalination applications. *Sep. Purif. Technol.*, 75(2), 87-101. <http://dx.doi.org/10.1016/j.seppur.2010.07.021>
- UNEP (2012). 21 Issues for the 21st Century: Result of the UNEP Foresight Process on Emerging Environmental Issues. Nairobi, Kenya: U. N. E. P. (UNEP) <http://www.unep.org/publications/ebooks/ForesightReport/>.
- Vrijenhoek, E.M., Hong, S., and Elimelech, M. (2001). Influence of membrane surface properties on initial rate of colloidal fouling of reverse osmosis and nanofiltration membranes. *J. Membr. Sci.*, 188(1), 115-128. [http://dx.doi.org/10.1016/S0376-788\(01\)00376-3](http://dx.doi.org/10.1016/S0376-788(01)00376-3)
- Wang, S., and Huang, G.H. (2014). An integrated approach for water resources decision making under interactive and compound uncertainties. *Omega*, 44(0), 32-40. <http://dx.doi.org/10.1016/j.omega.2013.10.003>
- Wang, S., and Huang, G.H. (2015). A multi-level Taguchi-factorial two-stage stochastic programming approach for characterization of parameter uncertainties and their interactions: An application to water resources management. *Eur. J. Oper. Res.*, 240(2), 572-581. <http://dx.doi.org/10.1016/j.ejor.2014.07.011>
- Wang, S., Huang, G.H., and Veawab, A. (2013a). A sequential factorial analysis approach to characterize the effects of uncertainties for supporting air quality management. *Atmos. Environ.*, 67(0), 304-312. <http://dx.doi.org/10.1016/j.atmosenv.2012.10.066>
- Wang, S., Huang, G.H., Wei, J., and He, L. (2013b). Simulation-based variance components analysis for characterization of interaction effects of random factors on Trichloroethylene vapor transport in unsaturated porous media. *Ind. Eng. Chem. Res.*, 52(25), 8602-8611. <http://dx.doi.org/10.1021/ie4012003>
- World Bank. (2009). *Assessment of Restrictions on Palestinian Water Sector Development: West Bank and Gaza*, Washington D.C.
- Zhao, Y., Hu, X.M., Jiang, B.H., and Li, L. (2014). Optimization of the operational parameters for desalination with response surface methodology during a capacitive deionization process. *Desalination*, 336(0), 64-71. <http://dx.doi.org/10.1016/j.desal.2013.12.024>
- Zhu, A., Christofides, P.D., and Cohen, Y. (2009). Minimization of energy consumption for a two-pass membrane desalination: Effect of energy recovery, membrane rejection and retentate recycling. *J. Membr. Sci.*, 339(1-2), 126-137. <http://dx.doi.org/10.1016/j.memsci.2009.04.039>
- Zulkali, M.M.D., Ahmad, A.L., and Derek, C.J.C. (2005). Membrane application in proteomic studies: Preliminary studies on the effect of pH, ionic strength and pressure on protein fractionation. *Desalination*, 179(1-3), 381-390. <http://dx.doi.org/10.1016/j.desal.2004.11.084>